J. Chem. Sci. (2021) 133:84
https://doi.org/10.1007/s12039-021-01933-2

REGULAR ARTICLE

An efficient $Ti_{0.95}Cu_{0.05}O_{1.95}$ catalyst for *ipso* – hydroxylation of arylboronic acid and reduction of 4-nitrophenol

SHRIKANTH K BHAT[a,b], PRASANNA[a], JAGADEESH PRASAD DASAPPA[b,*] and M S HEGDE[a,*]

[a]Talent Development Centre, Indian Institute of Science Challakere Campus, Chitradurga 577536, India
[b]Department of Chemistry, Mangalore University, Mangalagangotri, Konaje, Mangalore 574199, India
E-mail: jp_das@yahoo.com; jprasad2003@gmail.com; mshegde@iisc.ac.in

MS received 1 February 2021; revised 3 May 2021; accepted 4 May 2021

Abstract. A stable, active and selective $Ti_{0.95}Cu_{0.05}O_{1.95}$ catalyst, crystallized in anatase TiO_2 structure with 5% Cu^{2+} ions substituted for Ti^{4+} ions with 5% oxide ion vacancy has been synthesized by solution combustion method. The catalyst was coated over a cordierite monolith ($Mg_2Al_4Si_5O_{18}$) by solution combustion method. By the first principle density functional theory (DFT) calculations, 48 atoms bulk structure has been optimized and density of states (DOS) has been calculated. Ti – O bond distribution in $Ti_{0.95}Cu_{0.05}O_{1.95}$ has been compared with pure TiO_2. Bond distribution analysis has shown longer Cu – O and Ti – O bonds compared to those in CuO and TiO_2 creating Cu^{2+} and oxide ion vacancy as electrophilic and nucleophilic active sites, respectively. This catalyst was found to be very active for *ipso* – hydroxylation of arylboronic acid and 4-nitrophenol reduction reactions at room temperature. Catalyst coated cordierite monolith was used in the recycling process of the reaction for 20 cycles and cumulative turnover frequency was found to be 184,840 h^{-1}. $Ti_{0.95}Cu_{0.05}O_{1.95}$ catalyst coated on cordierite monolith enhanced the rate of the reaction compared to powder catalyst and made the handling and recycling of the catalyst very easy.

Keywords. Cordierite monolith; $Ti_{0.95}Cu_{0.05}O_{1.95}$; *Ipso* – hydroxylation; Nitro reduction; Density functional theory.

1. Introduction

Phenols and their derivatives have numerous applications in agrochemicals, pharmaceuticals, polymers and natural oxidants.[1] The development of methods to synthesize phenols are important especially in presence of many functional groups. As a result, establishing practical, general and efficient catalytic methods for the synthesis of phenols remains an area of tremendous research efforts. There are many methods to synthesize phenols that have some limitations such as harsh reaction conditions, low yield and more reaction time.[2] Hydroxylation of aryl bromides and chlorides has been reported using a palladium-based catalyst in presence of phosphine ligands.[3] Aryl iodide can also be converted into phenols in presence of copper-based catalyst using non-phosphine ligands at a higher temperature.[4] However, the availability of a wide range of arylboronic acid derivatives, their harmless nature, stability toward heat, air and moisture made them unique precursors for the synthesis of phenols.[5,6] There are a number of existing protocols, but a majority of the protocols have disadvantages like requirement of base, supports and additives, high temperature, long reaction time, oxygen atmosphere and lack of recyclability.[7,8]

Nitrophenols (NPs) are carcinogenic and extremely toxic for the environment and human health, as it is one of the stubborn water contaminants.[9,10] Among the nitrophenols, 4-NP has been verified to be risky for the liver, kidney, the central nervous system and the blood of both animal and human.[11] It is a challenging task to eliminate 4-NP from the environment.[12] Reduction of 4-NP is a possible reaction for synthesizing 4-aminophenol (4-AP) which is utilized as an intermediate for producing a large number of analgesic

*For correspondence

Supplementary Information: The online version contains supplementary material available at https://doi.org/10.1007/s12039-021-01933-2.

Published online: 07 August 2021

and antipyretic medicines (paracetamol, phenacetin, etc.).[13] Thus, an effective method for removing and utilizing 4-NP is the catalytic reduction of 4-NP to 4-AP. The application of sodium borohydride ($NaBH_4$) for reducing 4-NP in the presence of metal nanoparticles as catalysts has been a great countermeasure as this technique was first applied for treating 4-NP with Ag nanoparticles.[14] As a consequence of their high specific surface area and high adsorption capacity,[15-17] several nanomaterials have been utilized for catalysing the 4-NP reduction. These can be categorized into three main groups of noble metals (Ag,[18] Au,[19] Pt,[20] Pd,[21] Ir,[22] etc.), non-noble metals (Cu,[23] Mn,[24] etc.) and carbon materials (graphene[25] and graphitic carbon nitride,[26] etc.).

When we talk about catalysis in organic synthesis, recovering and recycling of the catalyst are the main issues faced by the researchers. Heterogeneous catalysts have some advantage of easy-to-handle and stability over homogeneous catalysts but complete recovery of these catalysts is a tedious process such as filtration or centrifugation which leads to loss of expensive catalysts. Therefore, easily separable catalysts are highly desirable in organic synthesis. In this way, metal ions substituted in reducible oxides have overcome these issues in recent years. One such catalyst system is metal ion substituted TiO_2 ($Ti_{1-x}M_xO_{2-x}$) coated on cordierite monolith eliminating handling of powder catalyst.[27-29]

Most of the metal-doped TiO_2 reported in the literature are prepared by co-precipitation and wet impregnation method.[30,31] The solution combustion method is a good technique in producing metal substituted oxides.[32-35] Substitution of copper metal ions in TiO_2 was reported in 2004.[36] $Ti_{0.925}Cu_{0.075}O_{2-\delta}$ was synthesized by solution combustion method. This catalyst was used in the photo-catalytic dye degradation process. The activity of the catalyst was low compared to un-substituted TiO_2 as a photo-catalyst. Till date, this catalyst was not explored much for any of the catalytic reactions.

In this paper, we report synthesis and characterization of $Ti_{0.95}Cu_{0.05}O_{1.95}$ catalyst and its application in *ipso* – hydroxylation of arylboronic acid and reduction of 4-nitrophenol at room temperature. Density functional theory has been employed to determine the structure of $Ti_{0.95}Cu_{0.05}O_{1.95}$ system. The catalyst was coated over cordierite monolith honeycomb and used in the reactions as a catalyst cartridge. It is a unique method where the catalyst cartridge can be recovered easily. Recycling of the catalyst has been studied for *ipso* – hydroxylation of phenylboronic acid, which has shown very good catalytic activity for 20 cycles with high turnover frequency (TOF).

2. Experimental

2.1 *Synthesis of $Ti_{0.95}Cu_{0.05}O_{1.95}$ powder catalyst*

Copper substituted TiO_2 catalyst was synthesized by solution combustion method. Titanium tetraisopropoxide ($Ti(OC_3H_7)_4$), cupric nitrate ($Cu(NO_3)_2$) and glycine were taken as starting materials. 5.7 mL (19 mmol) of titanium tetraisopropoxide has been added to a 100 mL beaker containing about 60 mL of distilled water. A white precipitate was formed and settled at the bottom. Water was decanted from the beaker and the precipitate was left behind in the beaker. Concentrated nitric acid ($\sim$3 mL) was added slowly to the precipitate until the white particles completely dissolved in acid. This clear solution of titanyl nitrate was transferred to a 300 mL capacity crystallizing dish. 0.188 g of cupric nitrate (1 mmol) and 1.665 g of glycine (22.2 mmol) were mixed with titanyl nitrate and dissolved completely by using a minimum amount of distilled water ($\sim$15 mL); kept in a 350 °C pre-heated muffle furnace. After 20 min, the dish was removed from the furnace. The solid product obtained from the combustion was ground nicely to get fine powder; it was characterized by powder X-ray diffraction. The Combustion reaction is given by:

$$9(1-x)TiO(NO_3)_2 + 10C_2H_5NO_2 + 9xCu(NO_3)_2 \rightarrow 9Ti_{1-x}Cu_xO_{2-d} + 20CO_2 + 14N_2 + 25H_2O : \; x = 0.05.$$

X-ray diffraction pattern was recorded on a Philips X'Pert diffractometer at a scan rate of 0.1°/min from the 2θ angle 10° to 90°. The diffraction profile was refined by Rietveld refinement method.

2.2 *Coating of $Ti_{0.95}Cu_{0.05}O_{1.95}$ catalyst over cordierite monolith honeycomb*

Cordierite monolith honeycombs are in a cylindrical shape with 2.5 cm diameter and 1 cm height with 400 cells/inch made of $Mg_2Al_4Si_5O_{18}$ (weight of the monolith is around 3 to 4g). Before coating the catalyst over monolith, γ –Al_2O_3 was coated over monolith to increase the surface area and adhesion to TiO_2, this is called wash – coating. This process was done by the solution combustion method. A clear solution of 15 mmol of $Al(NO_3)_3$ and 9 mmol of glycine with a

minimum amount of water (~ 15 mL) was made and a pre-weighed monolith was dipped in the solution. The monolith was kept inside the furnace for combustion at 350 °C. After 20 min, the monolith was removed from the furnace and allowed to cool. Loosely held particles of γ –Al_2O_3 on monolith was removed by sonication process in water. The weight of the monolith was measured. This procedure was repeated until the weight of the coated γ –Al_2O_3 was 2 to 2.5% of cordierite monolith weight.

In the process of coating the catalyst, the solution of starting materials was made in a 100 mL capacity beaker as mentioned in the procedure of synthesis of powder catalyst. Alumina coated pre-weighed monolith was dipped in the solution and kept inside the preheated furnace at 350 °C for combustion. Monolith was removed from the furnace after 30 min, allowed to cool and sonicated to remove loosely held catalyst particles. Repeated the procedure until desired weight of catalyst was coated which is 25 mg. Each monolith is having parallel channels of square shape. Thus the high surface area is exposed to the reactants in the reactions. Images of cordierite monolith before and after coating the catalyst are given in supplementary, Figure S2, SI. Both powder catalyst and coated on cordierite were green in colour indicating Cu is in +2 oxidation state.

2.3 *Temperature programmed reduction (H_2 – TPR)*

Temperature programmed reduction of samples was carried out in a continuous flow quartz microreactor of length 25 cm and 0.4 cm internal diameter with 5% H_2/Ar flowing at 20 cm^3 min^{-1} with a linear heating rate of 5 °C min^{-1}. We carried out the experiment from 30 to 400 °C. In a typical experiment, 75 mg of the sample was taken in a quartz microreactor and both the ends were plugged with ceramic wool. The sample was kept inside a furnace and heated at a linear rate of 5 °C min^{-1} from 30 to 400 °C. The amount of hydrogen taken up was detected by a thermal conductivity detector (TCD).

2.4 *Ipso-hydroxylation of arylboronic acid*

Screening reactions and substrate scope were carried out in a 10 mL capacity screw cap vial. 300 mg of phenylboronic acid was taken in a vial, 15 mg of powder catalyst and 3 mL of water was added. Stirred the mixture for 2 min at room temperature, then 4.92 mmol of H_2O_2 was added to the same vial. The reaction was monitored using TLC. After completion of the reaction, the product was extracted using 20 mL diethyl ether and 20 mL × 3-time water work up. Products were isolated using petroleum ether and ethyl acetate by column chromatography; isolated products were characterized by ^{1}H NMR and ^{13}C NMR.

In the recycling process, reactions were carried out in a specially designed flask (Figure S4, SI). Instead of powder catalyst, the coated catalyst has been used in the reactions. 500 mg of phenylboronic acid was charged into the flask, magnetic bead and honeycomb monolith was placed inside the flask. Sufficient water was added in a way that the monolith was completely submerged inside the flask. Then added 8.2 mmol of H_2O_2 and continued the reaction. Reactions were monitored using TLC. After each cycle, honeycomb monolith was taken out from the flask, washed with water and hexane; dried in a hot air oven at 200 °C for 1 h. After drying, it was used for another cycle of reaction. In this way, we recycled the coated catalyst 20 times.

2.5 *4-NP reduction using $Ti_{0.95}Cu_{0.05}O_{1.95}$ catalyst coated cordierite monolith*

30 mL of 0.0001 M 4-nitrophenol (4-NP) was taken in a specially designed flask. 100 mg of sodium borohydride ($NaBH_4$) was added to the 4-NP solution and stirred the mixture at room temperature for 3 min. Initial UV – Vis spectra of the solution was recorded which is considered as at zero time. After recording the spectra, $Ti_{0.95}Cu_{0.05}O_{1.95}$ coated cordierite monolith was placed inside the flask. The reaction started immediately, as we could see the evolution of hydrogen gas inside the flask. During the reaction, at an interval of 20 s, absorbance values were recorded until the yellow colour of the mixture disappeared. After the reaction, cordierite monolith was removed from the flask, washed with distilled water and hexane; dried in a hot air oven at 200 °C for 1 hour and reused for another reaction.

3. Results and Discussions

3.1 *Characterization of $Ti_{0.95}Cu_{0.05}O_{1.95}$ catalyst – XRD and H_2 – TPR studies*

Rietveld refined profile of $Ti_{0.95}Cu_{0.05}O_{1.95}$ is shown in Figure 1. $Ti_{0.95}Cu_{0.05}O_{1.95}$ crystallizes in anatase TiO_2 structure. The pattern is refined to anatase TiO_2 (tetragonal, $I4_1/amd$, JCPDS no. 21 – 1272). The difference plot of the observed and calculated pattern was

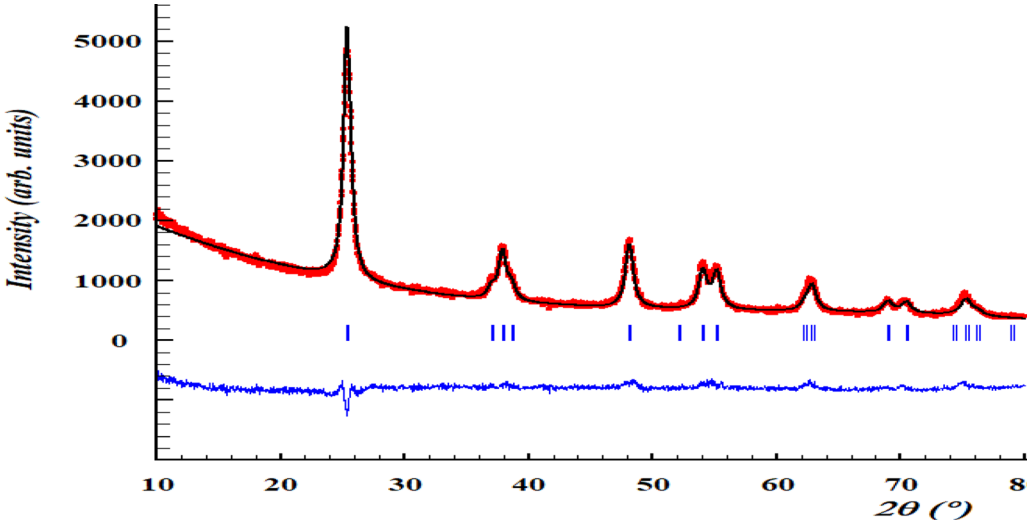

Figure 1. Rietveld refinement profile of $Ti_{0.95}Cu_{0.05}O_{1.95}$

almost a straight line which confirms 5 atom percentage of copper is substituted in TiO_2 without forming CuO. The difference plot did not show peaks due to CuO or Cu_2O indicating Cu ion is substituted in TiO_2. Lattice parameters were a = 3.779 Å, c = 9.489 Å. The structure reveals that for every Cu ion there is an oxide ion vacancy and Cu is in 5 coordination geometry. Ionic radius of Cu^{2+} (V) is 0.65 Å and that of Ti^{4+} (VI) is 0.605 Å. Since 5% of Cu^{2+} ion substituted in TiO_2, there is no significant change with lattice parameter of $Ti_{0.95}Cu_{0.05}O_{1.95}$ compared to TiO_2 anatase with a = 3.779 Å and c = 9.497 Å. The average crystallite size was calculated from the Scherrer formula; $d = 0.9\ \lambda/\beta\ \cos\theta$,[37] where λ is the wavelength of X-ray (Cu Kα), θ is the diffraction angle and β is the full-width half maxima (FWHM) in radians, calculated from $\beta = (u \tan^2\theta + v \tan\theta + w)^{1/2}$, where u, v and w values were obtained from Rietveld refinement. The average crystallite size of the catalyst is 8 nm.

H_2 uptake or H_2 – TPR by CuO and $Ti_{0.95}Cu_{0.05}O_{1.95}$ powders up to 400 °C are shown in Figure 2. H_2 molecule adsorbed on the catalyst reacts with lattice oxygen to produce water through the temperature-programmed reaction. The reactions can be written as follows:

$$CuO + H_2 \rightarrow Cu + H_2O$$

$$Ti_{0.95}Cu_{0.05}O_{1.95} + \delta H_2 \rightarrow Ti_{0.95}Cu_{0.05}O_{1.95-\delta}$$

On passing O_2 in the cooling cycle, we see, $Ti_{0.95}Cu_{0.05}O_{1.95-\delta} + \delta/2\ O_2 \rightarrow Ti_{0.95}Cu_{0.05}O_{1.95}$

Where, δ is the number of moles.

Firstly, H_2 – TPR of 3 mg of pure CuO was performed. Peaks observed at 265 °C and 320 °C indicate the reduction of CuO by H_2 to form copper metal (Figure 2a). Later, 75 mg of $Ti_{0.95}Cu_{0.05}O_{1.95}$ was taken and performed the H_2 – TPR experiment. A peak was observed at 180 °C, inferring the sample is reduced at that temperature by H_2 (Figure 2b). This peak corresponds to the reduction of Cu^{2+} to Cu^0. $Ti_{0.95}Cu_{0.05}O_{1.95}$ showed an oxygen storage capacity of 1020 µmol g^{-1}.

FT – IR analysis was carried out for $Ti_{0.95}Cu_{0.05}O_{2-\delta}$ catalyst (Figure 3). In comparison with TiO_2, the characteristic peaks due to –OH stretching frequencies of Cu/TiO_2 catalyst observed at 3422 and 1631 cm^{-1} which are having a comparably higher percentage of transmittance. One more characteristic peak observed at 1372 cm^{-1}. Below 800 cm^{-1}, a broad peak was observed corresponding to Ti – O – Ti vibrations. After the catalytic reaction, the used catalyst was once again subjected to FTIR analysis and it showed exactly the same characteristic peaks which were observed in freshly prepared catalyst confirming its structural integrity during the reaction.

3.2 *Density functional theory (DFT) studies of $Ti_{0.95}Cu_{0.05}O_{1.95}$ catalyst*

The total energy calculations were based on the Quantum Espresso[38] implementation of Density Functional Theory using the Generalized Gradient Approximation (GGA). Ultrasoft Pseudopotentials were used with Perdew-Burke-Ernzerhof (PBE) exchange-correlation. Single-particle Kohn−Sham

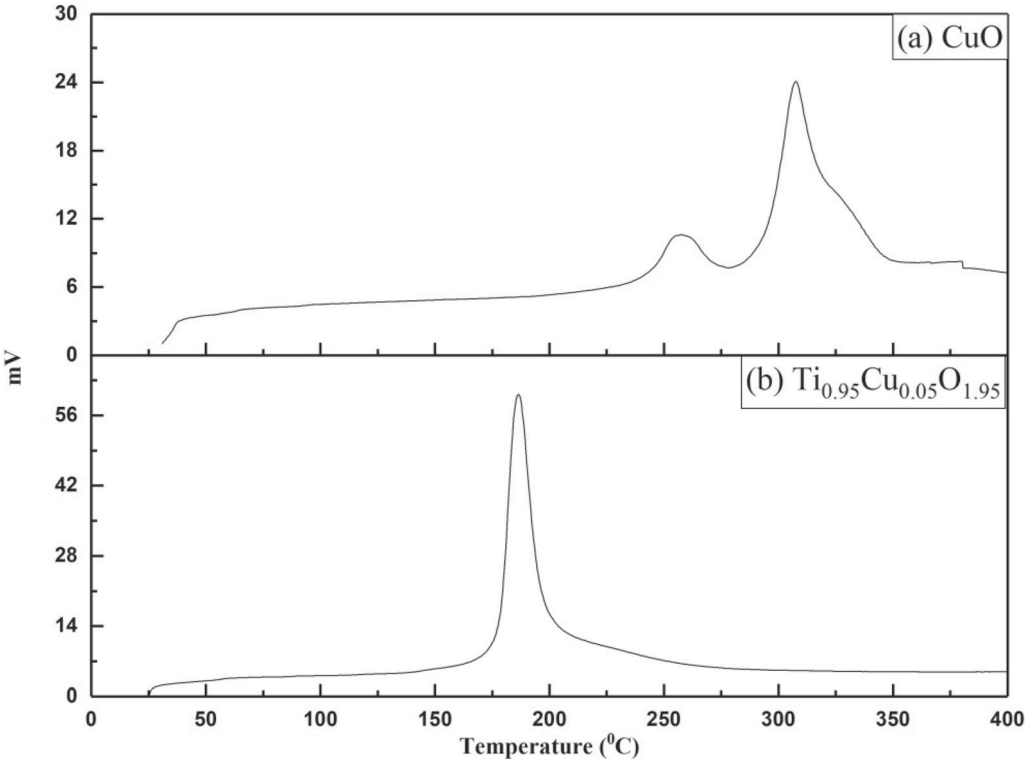

Figure 2. Temperature programmed reduction by Hydrogen (H_2 – TPR) plots of (a) CuO and (b) $Ti_{0.95}Cu_{0.05}O_{1.95}$.

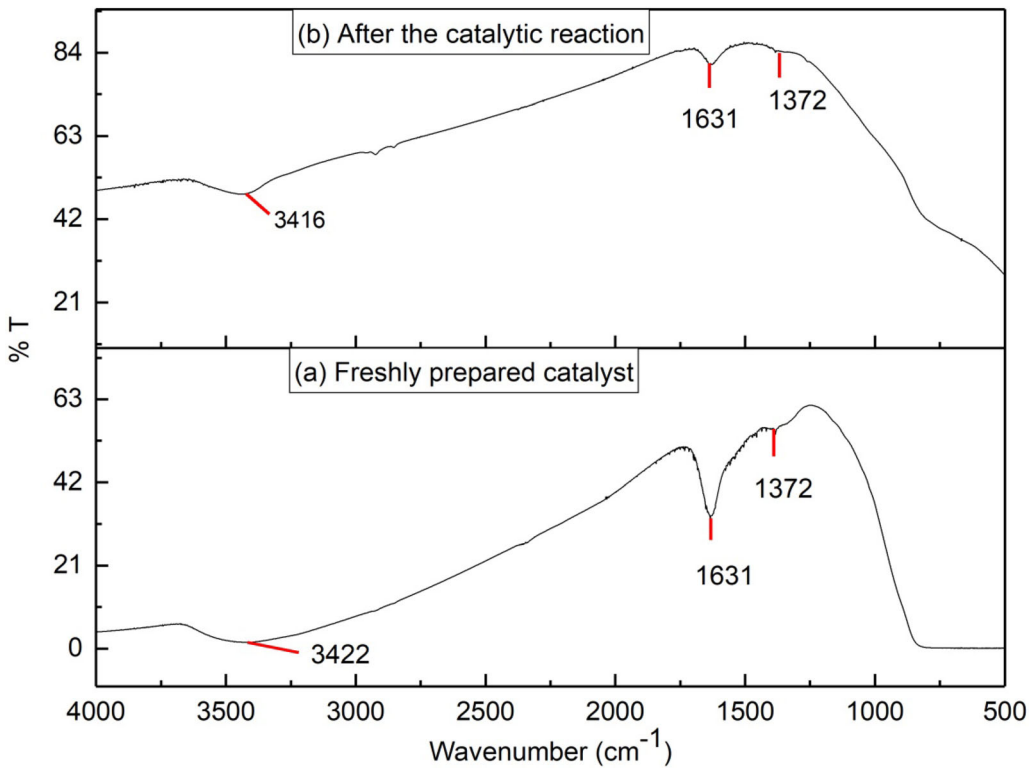

Figure 3. FT – IR spectra of (a) freshly prepared $Ti_{0.95}Cu_{0.05}O_{2-\delta}$ catalyst and (b) after the catalytic reaction

wave functions (density) were represented with a plane wave basis with an energy cut-off of 30 Ry (240 Ry).

We first simulated the structure of pure TiO_2 in anatase phase of 16 formula units. Cell parameters a = 3.846 Å and c = 9.6767 Å found using DFT are in agreement with the literature values.[39] Copper substituted TiO_2 was simulated by replacing one central Ti atom with Cu atom and one oxygen vacancy was created per Cu^{2+} ion substitution to compensate the net charge. The structure of $Ti_{15}Cu_1O_{31}$ was optimized until the energy accuracy of 10^{-6} eV was achieved. Integrals over the Brillouin zone were sampled on 4 × 4 × 4 k – point Monkhorst–Packmesh.[40] Local geometry of Cu ion was nearly square pyramidal, unlike Ti ion which is distorted octahedral. The optimized structure of the Cu/TiO_2 is given in Figure 4a. Cu substitution in TiO_2 was treated using periodic tetragonal supercells with 16 formula units (47 atoms) of anatase TiO_2. The lattice parameters of Cu/TiO_2 were a = 3.7999 Å and c = 9.6853 Å, which were close to the experimentally observed values. The projected density of states was calculated for TiO_2 and Cu/TiO_2 system provides valence band structure (Figure 5). The partial density of states for Cu (3d) indeed lies between the valence band and conduction of Cu/TiO_2.

The bond distances are obtained from the optimized structures. Bond distributions in pure TiO_2 and Cu/TiO_2 are given in Figure 6. In pure TiO_2, there are two types of bonds with bond distances 1.97 and 2.0 Å in 2:1 ratio, whereas, in Cu/TiO_2, bond distribution of Ti – O bonds range from 1.76 to 2.16 Å and Cu – O bond distances are at 1.93 (2 bonds), 1.96, 2.04 and 2.16 Å (Figure 4b). Bond valences of Ti – O bond in TiO_2 and Cu/TiO_2 were calculated using the formula, $s = \left(\frac{R}{R_o}\right)^{-N}$ and that of Cu – O bond was calculated using the formula $s = exp\left[\frac{(R_0-R)}{B}\right]$, where R and R_0 are the observed and actual bond lengths respectively and N = 5.2 and B = 0.4 are the fixed parameters.[39] Valences of Ti and Cu ions were calculated as the summation of individual bond valences ($V = \Sigma s_i$). Observed valences of Ti ion in pure TiO_2 and Cu/TiO_2 are 3.73 and 3.92, respectively and that of Cu ion is 1.81. The lower bond valence of Cu indicates higher reducibility of Cu^{2+} ion in the catalyst.[41] That is exactly observed in H_2-TPR experiment (Figure 2) where Cu^{2+} ion reduction peak shifted from 320 (in pure CuO) to 180 °C (in Cu/TiO_2). Length of Cu – O bonds observed in the DFT calculations also support the experimental observations.

3.3 *Screening and substrate scope for ipso – hydroxylation of arylbronic acids*

Freshly synthesized $Ti_{0.95}Cu_{0.05}O_{1.95}$ catalyst powder was used in *ipso*-hydroxylation of arylboronic acid reaction. Phenylboronic acid was taken as a model substrate for screening the reactions. 121.9 mg of phenylboronic acid (1 mmol, 1 equiv.) was taken in a 10 mL capacity reaction vial. 2 mL of hydrogen peroxide (30% v/v) and 6 mg (5 weight percentage to phenylboronic acid) of catalyst were added to the same vial and allowed to stir at room temperature without adding any solvent. The reaction was monitored by using TLC. Interestingly, within 4 min, the reaction was completed and furnished phenol in 100% yield (Table 1, entry 1). The next reaction was performed without the catalyst, we kept the reaction up to 5 h but only 35% of the reaction was completed (Table 1, entry 2). The reaction without any oxidant in water as solvent was unsuccessful (Table 1, entry 3). When UV light was irradiated on the reaction mixture; no product was observed (Table 1, entry 4). Instead of hydrogen peroxide, $K_2S_2O_8$ was used as an oxidant, 56% of the product was observed after 10 min

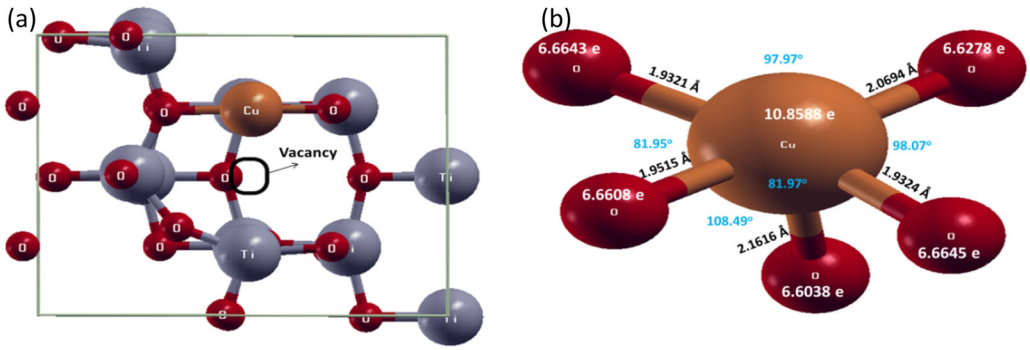

Figure 4. (a) 1 atom substituted in 16 formula units of Cu/TiO_2 bulk ($Ti_{15}Cu_1O_{31}$) with one oxide ion vacancy, (b) geometry of Copper in $Ti_{15}Cu_1O_{31}$

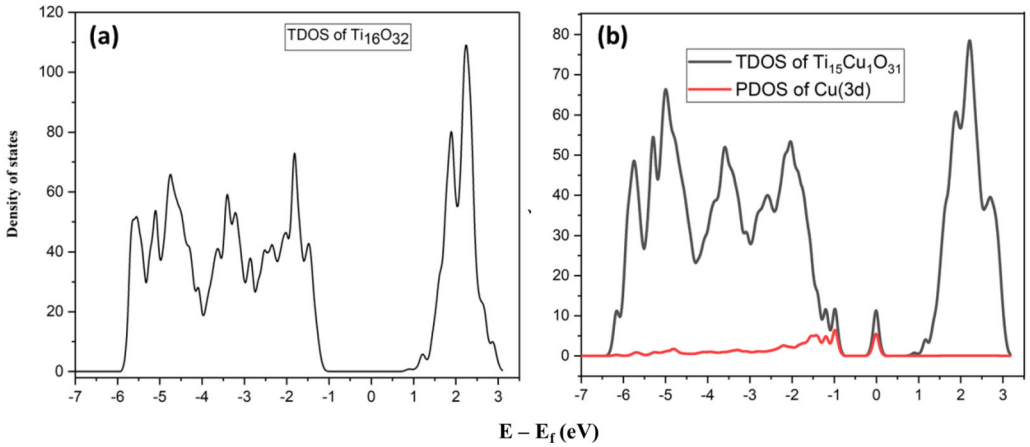

Figure 5. Total density of states (TDOS) of (a) TiO_2 and (b) $Ti_{0.95}Cu_{0.05}O_{1.95}$

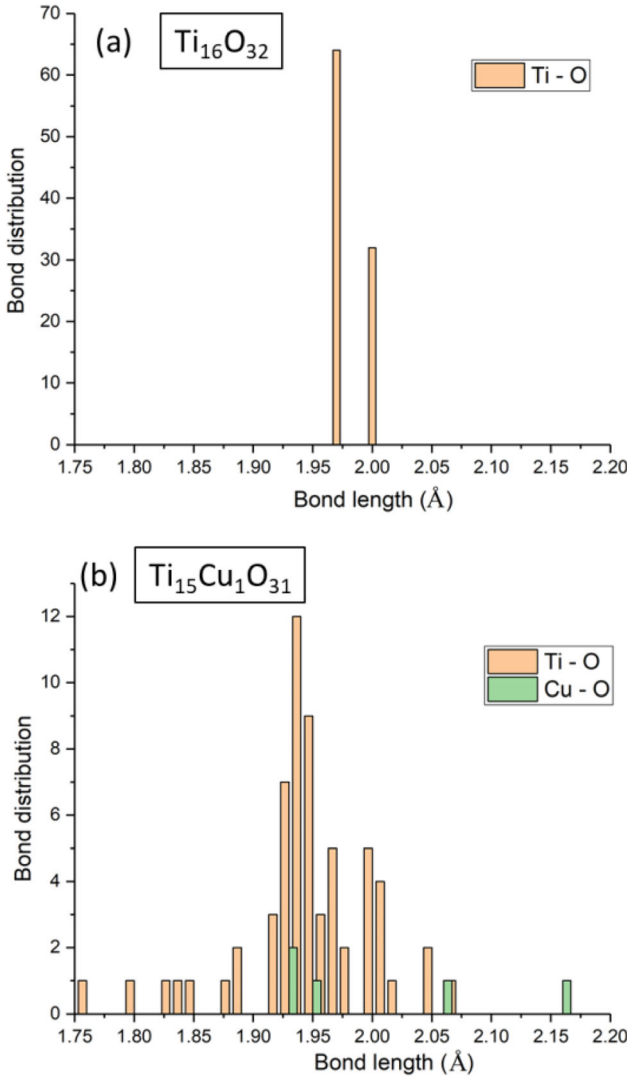

Figure 6. Bond distribution chart calculated for (a) $Ti_{16}O_{32}$ and (b) $Ti_{15}Cu_1O_{31}$

(Table 1, entry 5). We thought of screening the amount of H_2O_2 in the reaction. So we performed the reaction

Table 1. Screening study of *ipso*-hydroxylation of phenylboronic acid[a]

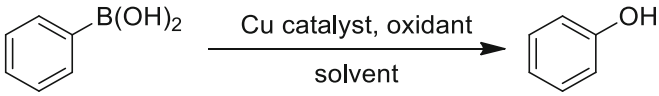

1a **2a**

Entry	Oxidant	Solvent	Time (min)	Yield (%)[b]
1	H_2O_2	–	3 – 4	100
2	H_2O_2	–	300	35[c]
3	–	H_2O	10	Trace
4	(UV)	H_2O	10	Trace
5	$K_2S_2O_8$	H_2O	10	56
6	H_2O_2	H_2O	6	100[d]
7	H_2O_2	H_2O	4	100[e]
8	H_2O_2	H_2O	4	100[f]
9	H_2O_2	H_2O	30	95[g]

[a]Reaction condition: 1 mmol of phenylboronic acid (121.9 mg, 1 equiv.), 5 weight percentage of catalyst (6 mg), 3 mL of H_2O_2, 1.1 equiv. of $K_2S_2O_8$, UV irradiation from 254 nm UV source. [b]All are isolated yield. [c]without catalyst. [d]1 mmol of H_2O_2 (1 equiv.). [e]2 mmol of H_2O_2 (2 equiv.). [e]3 mmol of H_2O_2 (3 equiv.). [g]2 mmol of H_2O_2 (2 equiv.), TiO_2 (6 mg) catalyst.

in water (3 mL) by adding a small amount of H_2O_2. To 1 mmol of phenylboronic acid and 6 mg of catalyst in water, 1 mmol of H_2O_2 was added. To our delight, the reaction was completed within 6 min to furnish phenol (Table 1, entry 6). By taking 2 mmol and 3 mmol of the H_2O_2, the reaction furnished phenol within 4 min (Table 1, entry 7 and 8). Instead of Cu – catalyst, we used 5 weight percentage of pure TiO_2 as a catalyst, reaction furnished phenol in 30 min with 95% yield (Table 1, entry 9). Compare to pure TiO_2,

Cu – substituted TiO_2 showed better result towards ipso – hydroxylation of phenylboronic acid. So we decided entry 7 as a standard reaction condition for substrate scope of *ipso* – hydroxylation reactions. TOF of the catalyst was 5440 h^{-1} which is quite remarkable.

Screening of the amount of catalyst has been performed under standard conditions. Series of reactions were performed starting from 0.5 weight percentage (0.6 mg) to 20 weight percentage (12 mg) catalyst with respect to the amount of phenylboronic acid (Figure S3, SI). This figure shows the TOF vs. weight percentage of the catalyst. When we took 0.5 weight percentage of catalyst, reaction completed after 90 min and TOF was 2976 h^{-1}. We increased the catalyst weight percentage to 1 and the reaction completed after 65 min. Until 4 weight percentage, TOF was around 2000–3000 h^{-1}. For 5 weight percentage of the catalyst, TOF had increased to 5357 h^{-1}. This reaction took 4 min to furnish phenol. The weight percentage of the catalyst was further increased to 10, 15 and 20 and the time taken to complete the reactions was 5 min in each case. But TOF decreased as can be seen in Figure S3, SI. This means, 5 weight percent of the catalyst is optimum for this reaction.

To evaluate the scope of the current protocol, a wide range of substituted arylboronic acids were examined under optimized reaction conditions using $Ti_{0.95}Cu_{0.05}O_{1.95}$ catalyst. It has been observed that the electronic nature and position of the substituents had very little effect on the reaction process. The results are summarized in Table 2. Despite having various substituents, all the arylboronic acids gave 100% conversion under 15 min. We have performed the conversion of 2- methyl phenylboronic acid to corresponding phenol **2b** (Table 2, entry 2) under 5 min, with 100% yield. TOF found to be 4752 h^{-1} for this reaction. Halogen substituted phenylboronic acids such as 4-fluoro, 3-chloro, 4-bromo and 4-iodo phenyboronic acids furnished corresponding phenols **2c**, **2d**, **2e** and **2f** in 100% yields respectively (Table 2, entry 3-6). In the next set of reactions, 2-, 3- and 4-substituted nitro phenylboronic acids (Table 2, entry 7-9) were converted into corresponding phenols **2g, 2h** and **2i** in 100% yields under 8 to 15 minutes. TOF calculated for all the reactions which range from 1290 to 6627 h^{-1}.

3.4 *Recycling of the catalyst in ipso-hydroxylation reaction*

Recycling of the catalyst was performed under standard reaction conditions. In this study, the cartridge catalyst method was used. Instead of powder catalyst, the catalyst was coated over cordierite monolith and used in the reactions. Monolith is coated with 25 mg of catalyst. A specially designed flask was used for these reactions. Charged phenylboronic acid (500 mg, 4.09 mmol) into the reaction flask followed by 15 mL of water. Placed catalyst coated monolith inside the reaction flask, stirred for 2 minutes and then added 2 equivalent of H_2O_2 (8.196 mmol, 83.6 mg). To our delight, after adding H_2O_2, the reaction completed within 2 min in the first cycle. It took half the time compared to the powder catalyst to complete the reaction, the reason being, more catalysts are exposed to reactants in this method due to the larger surface area of the cordierite monolith. The reaction was monitored by TLC and the product was extracted using diethyl ether and water work up. After each cycle of reaction, cordierite monolith was removed from the flask, washed with distilled water and hexane to remove hydrogen peroxide as well as organic impurities. Washed monolith was dried in a hot air oven at 200 °C for one hour. The dried monolith was reused in the next cycle of the reaction. The catalyst was recycled up to 20 times without any drop in the yield, each time reaction afforded 100% yield. Time taken for the reaction was 2 minutes at first cycle and 5 min at the 20th cycle. There might be leaching of copper catalyst from the cordierite monolith to a small extent. This is the reason why the reaction is taking a long time after several cycles. The average TOF of the monolith catalyst (in 20 recycles) was 9242 h^{-1} which is almost twice that of powder catalyst.

3.5 *Catalytic reduction of 4-nitro phenol*

To evaluate the robustness of the present catalyst, the reduction of 4- nitrophenol by $NaBH_4$ in presence of $Ti_{0.95}Cu_{0.05}O_{1.95}$ catalyst was investigated. To evaluate the catalyst activity quantitatively, we have performed a reduction of 4-NP to 4-AP by taking an excess amount of $NaBH_4$ under room temperature. Here, cordierite monolith catalyst was employed and the reaction was performed in a specially designed flask (Figure S5, SI). UV – Visible absorption spectra of 4-NP showed a strong absorption band at 317 nm (Figure S5, SI). Upon adding $NaBH_4$ to the solution of 4-NP, the strong absorption band had shifted from 317 to 400 nm (Figure S6, SI) due to the formation of 4-nitrophenolate ion in alkaline condition. The absorption band was unchanged almost for 1 h of stirring the mixture of 4-NP and $NaBH_4$ which indicates that reduction did not happen in absence of the catalyst.

Table 2. Substrate scope for *ipso* – hydroxylation reaction[a]

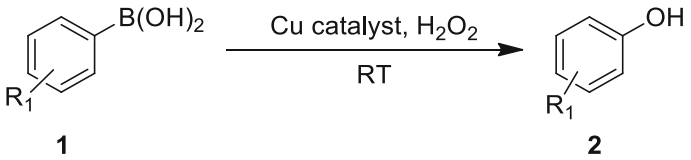

1 **2**

Entry	$ArB(OH)_2$	Product	Time (min)	TOF (h^{-1})
1	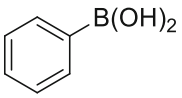	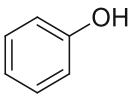 **2a**	4	6627
2	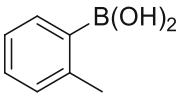	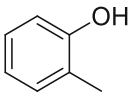 **2b**	5	4752
3	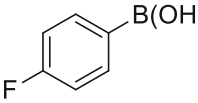	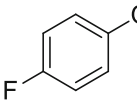 **2c**	4	5774
4	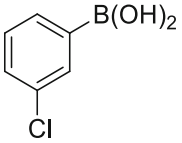	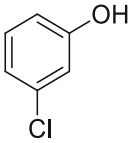 **2d**	6	4191
5	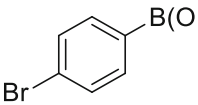	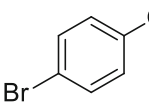 **2e**	8	2012
6	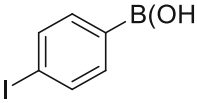	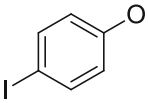 **2f**	6	2172
7	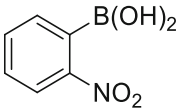	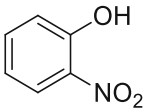 **2g**	15	1290
8	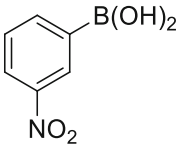	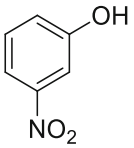 **2h**	8	2418
9	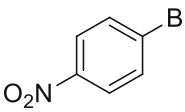	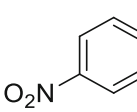 **2i**	10	1935

[a]Reaction conditions: 300 mg of arylboronic acid (1 equiv., 2.459 mmol), 15 mg of catalyst (5 weight percentage), 2 equiv. of H_2O_2 (4.92 mmol), 7 mL water, RT. All are isolated yields. TOF = (number of moles of product/number of moles of active site in the catalyst)/time in hours

When the catalyst is added to the reaction mixture, absorbance at 400 nm gradually decreased until 3 minutes as shown in the first cycle of Figure S7, SI. The pale green colour of the reaction mixture disappeared gradually during the catalytic reaction (Figure S5, SI). UV – Vis absorption spectra of solution of before reaction and after the reaction was recorded (Figure S6, SI). At 300 nm, a new absorption peak indicates the formation of 4-AP. In this reduction reaction, the concentration of $NaBH_4$ was large in

excess of that of 4-NP. So the reaction can be considered as a pseudo-first-order reaction. Therefore, reaction kinetics can be described as $\ln\left(\frac{A}{A_0}\right) = -kt$, where, k is first-order rate constant (s^{-1}), t is the reaction time, A and A_0 are absorbance values at time t and 0, since the ratio of absorbance at time t (A_t) to that of time t = 0 (A_0) should be equal to the concentration ratio $\left(\frac{C}{C_0}\right)$ for 4 – NP. A linear relationship between reaction time and $\ln(A/A_0)$ could be obtained in the reduction catalysed with $Ti_{0.95}Cu_{0.05}O_{1.95}$ (Figure 7a), and the rate constant k was 19.6×10^{-3} s^{-1}.

After the reaction, cordierite monolith was removed from the reaction flask, washed thoroughly with distilled water and hexane and dried in a hot air oven at 200 °C for 1 h. Dried cordierite monolith catalyst was ready for another reaction. In the 2nd cycle of the reduction reaction, the same experimental procedure was followed as explained above. The rate constant obtained for the 2nd cycle of the reaction was 18.46×10^{-3} s^{-1}, which is slightly lower than that of the 1st cycle reaction (Figure 7b). Similarly, the catalyst was recycled for 4 cycles and the corresponding rate constant values are given in Figure 7. Rate constant values are not changed much after 4 cycles of reaction which indicates, the catalyst is still active and stable.

3.6 *Mechanisms for ipso – hydroxylation and nitro reduction reactions*

A plausible mechanism for *ipso* – hydroxylation of arylboronic acid is depicted in Scheme 1. In the first step, hydrogen peroxide gets adsorbed on Cu ion to form a complex A. This complex reacts with phenylboronic acid with the removal of boric acid to form an adduct B. Finally, phenol moiety formed in the complex get detached from the catalyst and the catalyst will be ready for the next run.

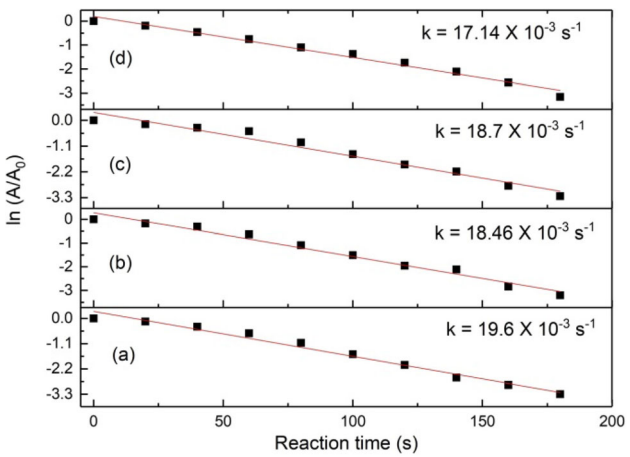

Figure 7. Plot of $\ln(A/A_0)$ against the reaction time for the reduction reaction of 4-NP by $NaBH_4$ using $Ti_{0.95}Cu_{0.05}O_{1.95}$ catalyst. Rate constant values are given for (a) 1st cycle, (b) 2nd cycle, (c) 3rd cycle and (d) 4th cycle reaction

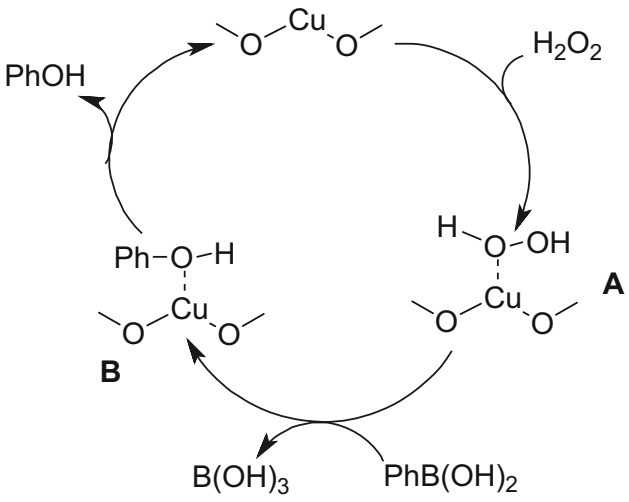

Scheme 1. Mechanisms for ipso – hydroxylation reaction

The mechanism for nitro reduction is depicted in Scheme 2. In the reaction, 3 molecules of H_2 are utilized and 2 molecules of water are liberated. In the first step, oxygen of nitrobenzene is adsorbed on the oxide ion vacancy site and hydrogen is adsorbed on the Cu^{2+} site. Rearrangement of this complex happens in such a way that oxygen which occupies in the vacancy forms a bond to Cu ion with simultaneous dissociation of hydrogen molecule activated at Cu ion. On further rearrangement, one water molecule is liberated and nitroso intermediate is liberated. In the second step, nitroso compound adsorbs on the oxide ion vacancy and another molecule of hydrogen activates on the Cu ion. Then oxygen of the nitroso group forms a bond with the Cu ion followed by hydrogen dissociation at Cu ion. This leads to the formation of hydroxyl amine intermediate. In the third step, yet another hydrogen molecule is activated at Cu ion and by the rearrangement of electrons aniline and water are formed. Then the catalyst is regenerated and it is ready for next run.

3.7 *Comparison of efficiency of $Ti_{0.95}Cu_{0.05}O_{1.95}$ catalyst with other catalysts*

To evaluate the efficiency of the present catalyst, we have compared our results with other catalysts given in Table 3. Clearly, the present catalyst is far superior to those reported.[42-47]

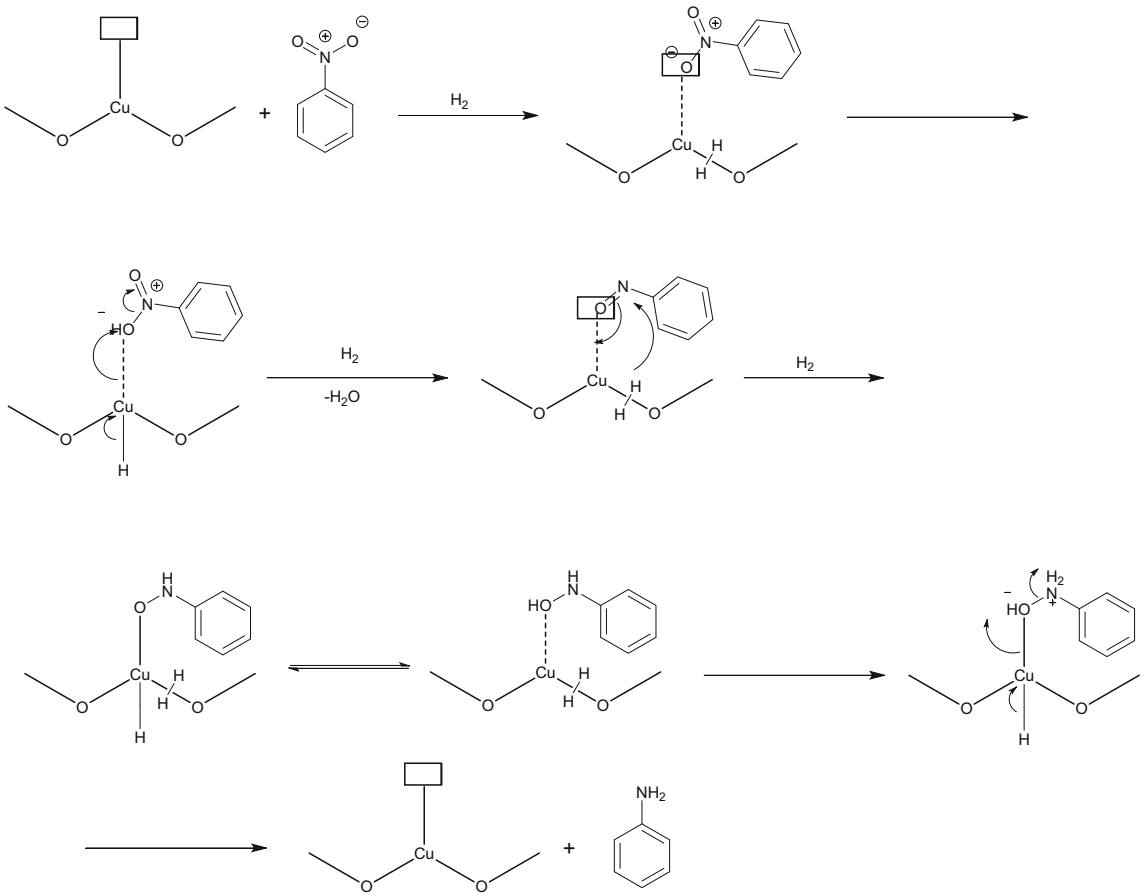

Scheme 2. Mechanisms for nitro reduction reaction

Table 3. Comparison of efficiency of various catalysts

Catalyst	Oxidant/additive	Solvent	Temperature (°C)	Time (min)	Yield (%)
5% Cu/TiO_2 (coated)	2 eq. 30% H_2O_2	3 mL water	RT	2	100 (this work)
Co-TCPP/PANI	TEA/Blue light	CH_3CN/H_2O	RT	360	90[42]
Cu/TCOP	H_2O_2	EtOH/water	RT	10	98[43]
$CuSO_4$/phen	KOH	water	RT	180	90[44]
-	$Na_2BO_3.4H_2O$ (sodium perborate) SPB	water	RT	5	92[45]
Cu_2O NPs	H_2O_2	water	RT	10	96[46]
CBPA	H_2O_2	water	RT	3	96[47]

4. Conclusions

In summary, $Ti_{0.95}Cu_{0.05}O_{1.95}$ catalyst was synthesized by solution combustion method and coated on cordierite monolith by dip-coating method. By first principle method DFT calculations, a 48 atoms bulk structure was simulated to understand the structure and bonding of the catalyst. The catalytic activity of this catalyst for *ipso*-hydroxylation of arylboronic acid and reduction of 4-nitrophenol reactions were investigated. The coated catalyst was recycled for 20 cycles without much drop in the product yield, which indicates that this catalyst is highly stable under the chosen reaction conditions. This catalyst is expected to find more application in organic synthesis.

Supplementary Information (SI)

Supplementary information associated with this article and Figures S1-S7 and Table S1 are available at www.ias.ac.in/chemsci.

References

1. Tyman J H P 1996 *Synthetic and natural Phenols* (Elsevier: New York)
2. Hanson P, Jones J R, Taylor A B, Walton P H and Timms A W J 2002 Sandmeyer reactions. Part 7.1. An investigation into the reduction steps of Sandmeyer hydroxylation and chlorination reactions *J. Chem. Soc. Perkin Trans.* **2** 1135
3. Anderson K W, Ikawa T, Tundel R E and Buchwald S L 2006 The Selective reaction of aryl halides with KOH: Synthesis of phenols, aromatic ethers, and benzofurans *J. Am. Chem. Soc.* **128** 10694
4. Zhao D, Wu N, Zhang S, Xi P, Su X, Lan J and You J 2009 Synthesis of phenol, aromatic ether, and benzofuran derivatives by copper-catalyzed hydroxylation of aryl halides *J. Angew. Chem. Int. Ed.* **48** 8729
5. Toyao T, Ueno N, Miyahara K, Matsui Y, Kim T-H, Horiuchi Y, et al. 2015 Visible-light, photoredox catalyzed, oxidative hydroxylation of arylboronic acids using a metal–organic framework containing tetrakis(-carboxyphenyl)porphyrin groups *Chem. Commun.* **51** 16103
6. Yu X and Cohen S M 2015 Photocatalytic metal–organic frameworks for the aerobic oxidation of arylboronic acids *Chem. Commun.* **51** 9880
7. Mahanta A, Adhikari P, Bora U and Thakur A J 2015 Biosilica as an efficient heterogeneous catalyst for ipso-hydroxylation of arylboronic acids *Tetrahedron Lett.* **56** 1780
8. Gogoi A and Bora U 2012 An Iodine-promoted, mild and efficient method for the synthesis of phenols from arylboronic acids *Synlett* **23** 1079
9. Ahmed A B, Jibril B, Danwittayakul S and Dutta J 2014 Microwave-enhanced degradation of phenol over Ni-loaded ZnO nanorods catalyst *Appl. Catal. B Environ.* **156** 456
10. Dong Z P, Le X D, Dong C X, Zhang W, Li X L and Ma J T 2015 Ni@Pd core–shell nanoparticles modified fibrous silica nanospheres as highly efficient and recoverable catalyst for reduction of 4-nitrophenol and hydrodechlorination of 4-chlorophenol *Appl. Catal. B Environ.* **162** 372
11. Bukowska B, Michalowicz J, Krokosz A and Sicinska P 2007 Comparison of the effect of phenol and its derivatives on protein and free radical formation in human erythrocytes (in vitro) *Blood Cells Mol. Dis.* **39** 238
12. Kong X K, Sun Z Y, Chen M, Chen C L and Chen Q W 2013 Metal-free catalytic reduction of 4-nitrophenol to 4-aminophenol by N-doped grapheme *Energy Environ. Sci.* **6** 3260
13. Chinnappan A, Tamboli A H, Chung W J and Kim H 2016 Green synthesis, characterization and catalytic efficiency of hypercross-linked porous polymeric ionic liquid networks towards 4-nitrophenolreduction *Chem. Eng. J.* **285** 554
14. Pradhan N, Pal A and Pal T 2002 Silver nanoparticle catalyzed reduction of aromatic nitro compounds *Colloids Surf. A* **196** 247
15. Saleh T A 2016 Nanocomposite of carbon nanotubes/silica nanoparticles and their use for adsorption of Pb(II): from surface properties to sorption mechanism *Desalin. Water Treat.* **57** 10730
16. Saleh T A 2015 Mercury sorption by silica/carbon nanotubes and silica/activated carbon: a comparison study *J. Water Supply Res. T.* **64** 892
17. Saleh T A 2015 Isotherm, kinetic, and thermodynamic studies on Hg (II) adsorption from aqueous solution by silica- multiwall carbon nanotubes *Environ. Sci. Pollut. R.* **22** 16721
18. Ai L, Yue H and Jiang J 2012 Environmentally friendly light-driven synthesis of Ag nanoparticles in situ grown on magnetically separable biohydrogels as highly active and recyclable catalysts for 4-nitrophenol reduction *J. Mater. Chem.* **22** 23447
19. Liu R, Mahurin SM, Li C, Unocic R R, Idrobo J C, Gao H, et al. 2011 Dopamine as a carbon source: the controlled synthesis of hollow carbon spheres and yolk-structured carbon nanocomposites *Angew. Chem. Int. Ed.* **50** 6799
20. Coccia F, Tonucci L, Bosco D, Bressan M and d'Alessandro N 2012 One-pot synthesis of lignin-stabilised platinum and palladium nanoparticles and their catalytic behaviour in oxidation and reduction reactions *Green Chem.* **14** 1073
21. Mei Y, Lu Y, Polzer F, Ballauff M and Drechsler M 2007 Catalytic activity of palladium nanoparticles encapsulated in spherical polyelectrolyte brushes and core-shell microgels *Chem. Mater.* **19** 1062
22. Xu D, Diao P, Jin T, Wu Q, Liu X, Guo X, et al. 2015 Iridium Oxide Nanoparticles and Iridium/Iridium Oxide Nanocomposites: Photochemical Fabrication and Application in Catalytic Reduction of 4-Nitrophenol *ACS Appl. Mater. Interfaces* **7** 16738
23. Sun Y, Xu L, Yin Z and Song X 2013 Synthesis of copper submicro/nanoplates with high stability and their recyclable superior catalytic activity towards 4-nitrophenol reduction *J. Mater. Chem. A* **1** 12361
24. Pal J, Mondal C, Sasmal A K, Ganguly M, Negishi Y and Pal T 2014 Account of nitroarene reduction with size- and facet-controlled $CuO-MnO_2$ nanocomposites *ACS Appl. Mater. Interfaces* **6** 9173
25. Hu H, Xin J H, Hu H and Wang X 2015 Structural and mechanistic understanding of an active and durable graphene carbocatalyst for reduction of 4-nitrophenol at room temperature *Nano Res.* **8** 3992
26. Li X-H, Wang X and Antonietti M 2012 Mesoporous g-C_3N_4 nanorods as multifunctional supports of ultrafine metal nanoparticles: hydrogen generation from water and reduction of nitrophenol with tandem catalysis in one step *Chem. Sci.* **3** 2170
27. Bhat S K, Prasad J D and Hegde M S 2019 Recyclable Pd Ionic catalyst coated on cordierite monolith for high TOF Heck coupling reaction *J. Chem. Sci.* **131** 20

28. Bhat S K, Lanke V, Prasad J D and Prabhu K R 2020 Ligand-free Suzuki coupling reaction with highly recyclable ionic palladium catalyst, $Ti_{1-x}Pd_xO_{2-x}$ (x=0.03) *Appl. Catal. A Gen.* **596** 117516
29. Bhat S K, Prasanna Dasappa J P and Hegde M S 2020 Palladium ion catalysed oxidative C-C bond formation reactions in arylboronic acid: application of cordierite monolith coated catalyst *Catal. Lett.* **150** 2911
30. Di Paola A, Lopez E G, Ikeda S, Marci G, Ohatani B and Palmisano L 2002 Photocatalytic degradation of organic compounds in aqueous systems by transition metal doped polycrystalline TiO_2 *Catal. Today* **75** 87
31. Grzybowska B, Słoczynski J, Grabowski R, Samson K, Gressel I, Wcisło K, et al. 2002 Tetragonal structure, anionic vacancies and catalytic activity of SO_4^{2-}-ZrO_2 catalysts for *n*-butane isomerization *Appl. Catal. A Gen.* **230** 1
32. McFarland E W and Metiu H 2013 Catalysis by doped oxides *Chem. Rev.* **113** 4391
33. Priolkar K R, Bera P, Sarode P R, Hegde M S, Emura S, Kumashiro R and Lalla N P 2002 Formation of $Ce_{1-x}Pd_xO_{2-\delta}$ solid solution in combustion-synthesized Pd/CeO_2 catalyst: XRD, XPS, and EXAFS investigation *Chem. Mater.* **14** 2120
34. Bera P, Priolkar K R, Sarode PR, Hegde M S, Emura S, Kumashiro R and Lalla N P 2002 Structural investigation of combustion synthesized Cu/CeO_2 catalysts by EXAFS and other physical techniques: formation of a $Ce_{1-x}Cu_xO_{2-\delta}$ solid solution *Chem. Mater.* **14** 3591
35. Bera P, Gayen A, Hegde M S, Lalla N P, Spadaro L, Frusteri F and Aruna F 2003 Promoting effect of CeO_2 in combustion synthesized Pt/CeO_2 catalyst for CO oxidation *J. Phys. Chem. B* **107** 6122
36. Nagaveni K, Hegde M S and Madras G 2004 Structure and photocatalytic activity of $Ti_{1-x}M_xO_{2-\delta}$ (M = W, V, Ce, Zr, Fe, and Cu) synthesized by solution combustion method *J. Phys. Chem. B* **108** 20204
37. Cullity B D 1978 *Elements of X-ray Diffraction* 2nd edn. (Addison Wesley: Reading, MA)
38. Paolo G et al, 2009 "QUANTUM ESPRESSO: A Modular and open source software project for quantum simulations of materials" *J. Phys.: Condens. Matter* **21** 395502
39. Mukri B D, Dutta G, Waghmare U V and Hegde M S 2012 Activation of lattice oxygen of TiO_2 by Pd^{2+} ion: correlation of low-temperature CO and hydrocarbon oxidation with structure of $Ti_{1-x}Pd_xO_{2-x}$ (x = 0.01−0.03) *Chem. Mater.* **24** 4491
40. Monkhorst H J and Pack J D 1976 Special Points for Brillouin-zone integrations *Phys. Rev. B* **13** 5188
41. Venkatesan T, Inam A, Dutta B, Ramesh R, Hegde M S, Wu X D, et al. 1990 Epitaxial $Y_1Ba_2Cu_3O_{7-y}/Y_{1-x}Pr_xBa_2Cu_3O_{7-y}$ heterostructures *Appl. Phys. Lett.* **56** 391
42. Alaa A A and Kimura M 2020 Oxidative Hydroxylation of Aryl Boronic Acid Catalyzed by Co-porphyrin Complexes via Blue-Light Irradiation *Catalysts* **10** 1262
43. Velu S, Muniyasamy H, Ganesan E, Rajendran B, Sepperumal M and Ayyanar S 2020 Copper nanoparticles supported on highly nitrogen-rich covalent organic polymers as heterogeneous catalysts for the *ipso*-hydroxylation of phenyl boronic acid to phenol *New J. Chem.* **44** 6222
44. Xu J, Wang X, Shao C, Su D, Cheng G and Hu Y 2010 Highly Efficient Synthesis of Phenols by Copper-Catalyzed Oxidative Hydroxylation of Arylboronic Acids at Room Temperature in Water *Org. Lett.* **12** 1964
45. Yang X, Jiang X, Wang W, Yang Q, Ma Y and Wang K 2019 Catalyst- and solvent-free ipso-hydroxylation of arylboronic acids to phenols *RSC Adv.* **9** 34529
46. Borah R, Saikia E, Bora S J and Chetia B 2017 Banana pulp extract mediated synthesis of Cu_2O nanoparticles: An efficient heterogeneous catalyst for the *ipso*-hydroxylation of arylboronic acids *Tetrahedron Lett.* **58** 1211
47. Das S K, Tahu M, Gohain M, Deka D and Bora U 2020 Bio-based sustainable heterogeneous catalyst for *ipso*-hydroxylation of arylboronic acid *Sustain. Chem. Pharm.* **17** 100296